Evaluating the use of optimally respiratory gated 18F-FDG-PET in target volume delineation and its influence on radiation doses to the organs at risk in non-small-cell lung cancer patients

Wijsman, R.; Grootjans, W.; Troost, E.G.; Heijden, E.H. van der; Visser, E.P.; Geus-Oei, L.F. de; Bussink, J.

Original article

Nuclear Medicine Communications

Evaluating the use of optimally respiratory gated ^{18}F-FDG-PET in target volume delineation and its influence on radiation doses to the organs at risk in non-small-cell lung cancer patients

Robin Wijsman[a], Willem Grootjans[b], Esther G. Troost[f,g,h], Erik H. van der Heijden[c], Eric P. Visser[b], Lioe-Fee de Geus-Oei[d,e] and Johan Bussink[a]

Objective **This radiotherapy planning study evaluated tumour delineation using both optimally respiratory gated and nongated fluorine-18 fluorodeoxyglucose-PET (^{18}F-FDG-PET).**

Methods **For 22 non-small-cell lung tumours, both scans were used to create the nongated and gated (g) gross tumour volumes (GTVg) together with the accompanying clinical target volumes (CTV) and planning target volumes (PTV). The size of the target volumes (TV) was evaluated and the accompanying radiotherapy plans were created to study the radiation doses to the organs at risk (OAR).**

Results **The median volumes of GTVg, CTVg and PTVg were statistically significantly smaller compared with the corresponding nongated volumes, resulting in a median TV reduction of 0.5 cm^3 (interquartile range 0.1–1.2), 1.5 cm^3 (− 0.2 to 7.0) and 2.3 cm^3 (− 0.5 to 11.3) for the GTVg, CTVg and PTVg, respectively. For the OAR, only the percentage of lung (GTV included) receiving at least 35 Gy was significantly smaller after gating, with a median difference in lung volume receiving at least 35 Gy of 5.7 cm^3 (interquartile range − 0.8 to 30.50).**

Conclusion **Compared with nongated ^{18}F-FDG-PET, the TVs obtained with optimally respiratory gated ^{18}F-FDG-PET were significantly smaller, however, without a clinically relevant difference in radiation dose to the OAR.** ***Nucl Med Commun*** **37:66–73**

Nuclear Medicine Communications 2016, **37**:66–73

Keywords: ^{18}F-FDG-PET, non-small-cell lung cancer, radiotherapy, respiratory gating

Departments of [a]Radiation Oncology, [b]Radiology and Nuclear Medicine, [c]Pulmonary Diseases, Radboud University Medical Center, Nijmegen, [d]Department of Radiology, Leiden University Medical Center, Leiden, [e]Biomedical Photonic Imaging Group, MIRA Institute, University of Twente, Enschede, The Netherlands, [f]Institute of Radiooncology, Helmholtz-Zentrum Dresden-Rossendorf, [g]Department of Radiotherapy and Radiooncology, University Hospital Carl Gustav Carus at the Technische Universität Dresden and [h]OncoRay, National Center for Radiation Research in Oncology, Dresden, Germany

Correspondence to Robin Wijsman, MD, Department of Radiation Oncology 874, Radboud University Medical Center, PO Box 9101, Nijmegen 6500 HB, The Netherlands
Tel: + 31 24 3614515; fax: + 31 24 3610792;
e-mail: robin.wijsman@radboudumc.nl

Received 17 July 2015 **Accepted** 9 September 2015

Introduction

The overall survival rates for advanced stage non-small-cell lung cancer (NSCLC) remain poor [1]. Treatment intensification such as concurrent chemoradiotherapy showed some benefit compared with sequential regimens, increasing the 2-year overall survival from 30.3 to 35.6% at the cost of increased acute oesophageal toxicity [2]. For radiotherapy dose-escalation strategies with three-dimensional conformal radiotherapy, treatment-related toxicity is often the dose-limiting factor [3]. Compared with these older techniques, modern intensity-modulated radiation therapy and volumetric modulated arc therapy techniques enable more conformal high-dose irradiation of the tumour [4,5]. Hence, radiation dose escalation is possible at the cost of a limited increase in toxicity [6–8].

Besides improved radiotherapy delivery techniques, a better depiction of the primary tumour decreases uncertainties of tumour delineation, which may contribute towards smaller target volumes. Bradley *et al.* [9] showed that the gross tumour volume (GTV) as delineated on fluorine-18 fluorodeoxyglucose (^{18}F-FDG) PET was significantly smaller than the GTV derived from computed tomography (CT) alone. This increased accuracy of ^{18}F-FDG-PET tumour delineation was confirmed in studies comparing the delineated CT and ^{18}F-FDG-PET volumes with the pathology specimens [10,11]. Thus, ^{18}F-FDG-PET/CT incorporated into radiotherapy planning may contribute towards more conformal treatment plans. Moreover, ^{18}F-FDG-PET/CT can be used for functional response monitoring [12] and it provides the possibility to define certain tumour subvolumes harbouring unfavourable tumour characteristics (e.g. high-metabolic activity) that can be a specific target for radiotherapy dose escalation [13,14].

Because of the relatively long acquisition time of ^{18}F-FDG-PET, patients breathe freely during image

0143-3636 DOI: 10.1097/MNM.0000000000000409

acquisition. For lung tumours, this results in motion artefacts underestimating tracer uptake and overestimating the tumour volume [15]. To overcome this problem, several respiratory gating systems have been developed [16]. These systems usually rely on the simultaneous acquisition of a respiratory signal that is used to select specific parts of the ^{18}F-FDG-PET data corresponding to the same respiratory phase. This results in a decrease in respiratory motion from the ^{18}F-FDG-PET image showing reduced blurring of the tumour. Amplitude-based optimal respiratory gating in ^{18}F-FDG-PET imaging resulted in a significant increase in mean tracer uptake [17,18], with a concordant significant decrease in lesion volume, while maintaining good image quality [18]. This indicates that the use of gated ^{18}F-FDG-PET improves tumour visualization and the quantification of tumour volume, which is important in tumour staging, treatment response assessment and probably also for radiotherapy planning.

We hypothesize that the smaller target volumes obtained with gated ^{18}F-FDG-PET lead to smaller target volumes for radiotherapy planning and thus improve healthy tissue sparing. Therefore, we investigated the effect of amplitude-based optimally respiratory gated ^{18}F-FDG-PET imaging compared with conventional nongated ^{18}F-FDG-PET imaging on radiotherapy planning with respect to the radiation dose delivered to healthy tissues.

Methods

This retrospective study evaluated the added value of high-resolution optimally respiratory gated ^{18}F-FDG-PET imaging on radiotherapy planning. We used the diagnostic ^{18}F-FDG-PET scans of patients with NSCLC as acquired in the study by Grootjans *et al.* [18]. In 21 patients, 22 equally distributed primary tumours (eight upper lobe, eight lower lobe and six located at the lung hilum) were analysed showing the largest differences in the gated versus nongated tumour volumes. After coregistration with the low-dose CT scans, the ^{18}F-FDG-PET/CT images were transferred to the radiotherapy planning system Pinnacle^3 (Version 9.6; Philips Radiation Oncology Systems, Best, the Netherlands). Information on image acquisition and image reconstruction will be described briefly as more detailed information has been described elsewhere [18]. After administration of ^{18}F-FDG (adjusted to patients' weight; 3.2 ± 0.2 MBq/kg), whole-body ^{18}F-FDG-PET gated and nongated images covering the thorax and upper abdomen were acquired using a Siemens Biograph 40 mCT PET/CT scanner (Siemens Medical Solutions USA Inc., Knoxville, Tennessee, USA). The respiratory signal was obtained using an Anzai AZ-733V respiratory gating system (Anzai Medical Co., Tokyo, Japan). Respiratory gating of the PET data was performed using an optimal amplitude-based respiratory gating algorithm (HD·Chest) using 35% of the acquired PET data, providing a good balance between motion rejection and image quality [18]. For the purpose of attenuation correction, anatomical reference and radiotherapy planning, a free-breathing total-body low-dose CT was performed. The ^{18}F-FDG-PET images were reconstructed using the TrueX algorithm (Siemens Medical Solutions USA Inc.) with time of flight measurements incorporated. Image reconstruction was performed with three iterations, 21 subsets and a matrix size of 400×400 (2.04×2.04 mm).

All primary tumours were delineated twice: once using the nongated ^{18}F-FDG-PET images and once using the respiratory gated ^{18}F-FDG-PET images. To minimize intraobserver variation because of manual contouring, automatic delineation of the tumour was performed with a fixed threshold region growing segmentation algorithm. The threshold chosen to represent the GTV was 40% of the maximum standardized uptake value (40% SUV_{max}; Fig. 1) [19], which was checked visually for plausible segmentation results. According to the local protocol, a 10 mm circumferential margin for the clinical target volume (CTV) was added to both GTVng and GTVg (ng and g refer to nongated and gated, respectively). Organs at risk (OAR), that is healthy lung tissue (delineated twice, once including the GTV and once excluding the GTV), heart, oesophagus and spinal cord, were delineated as well (for detailed information, see the Materials and methods section in the study by Hoffmann *et al.* [8]) and subtracted from the CTV in case tumour involvement was absent. When the tumour was located near other healthy tissues such as the thoracic wall or spine, these noninvolved structures were manually delineated creating a single contour, which could also be subtracted from CTVng and CTVg. The planning target volume (PTV) was generated by expanding the CTVng and CTVg with a 5 mm circumferential margin. Although this margin may seem inappropriate (especially in the case of increased tumour motion), this approach was considered adequate for the evaluation of the added value of gated ^{18}F-FDG-PET imaging in radiotherapy planning. Treatment plans were generated for both the PTVng and the PTVg planning 66 Gy in 33 fractions using a volumetric modulated arc therapy technique. To avoid differences in outcome because of different planning strategies, all factors involved in treatment planning (such as beam angles, number of segments, objectives and constraints) were maintained equal for both treatment plans. A dose coverage of 99% for the 95% isodose for the PTV was aimed for. If a 99% coverage was not achieved because of unacceptable high doses to the OAR, a lower coverage was accepted to generate a clinically acceptable treatment plan. For both plans, the dose coverage for the PTV was equalized manually by adjusting the number of monitor units (which quantifies the amount of radiation delivered by the linear accelerator). Treatment plans were evaluated for the following endpoints: PTV dose coverage, maximum dose to the organ at risk (D_{max}),

Fig. 1

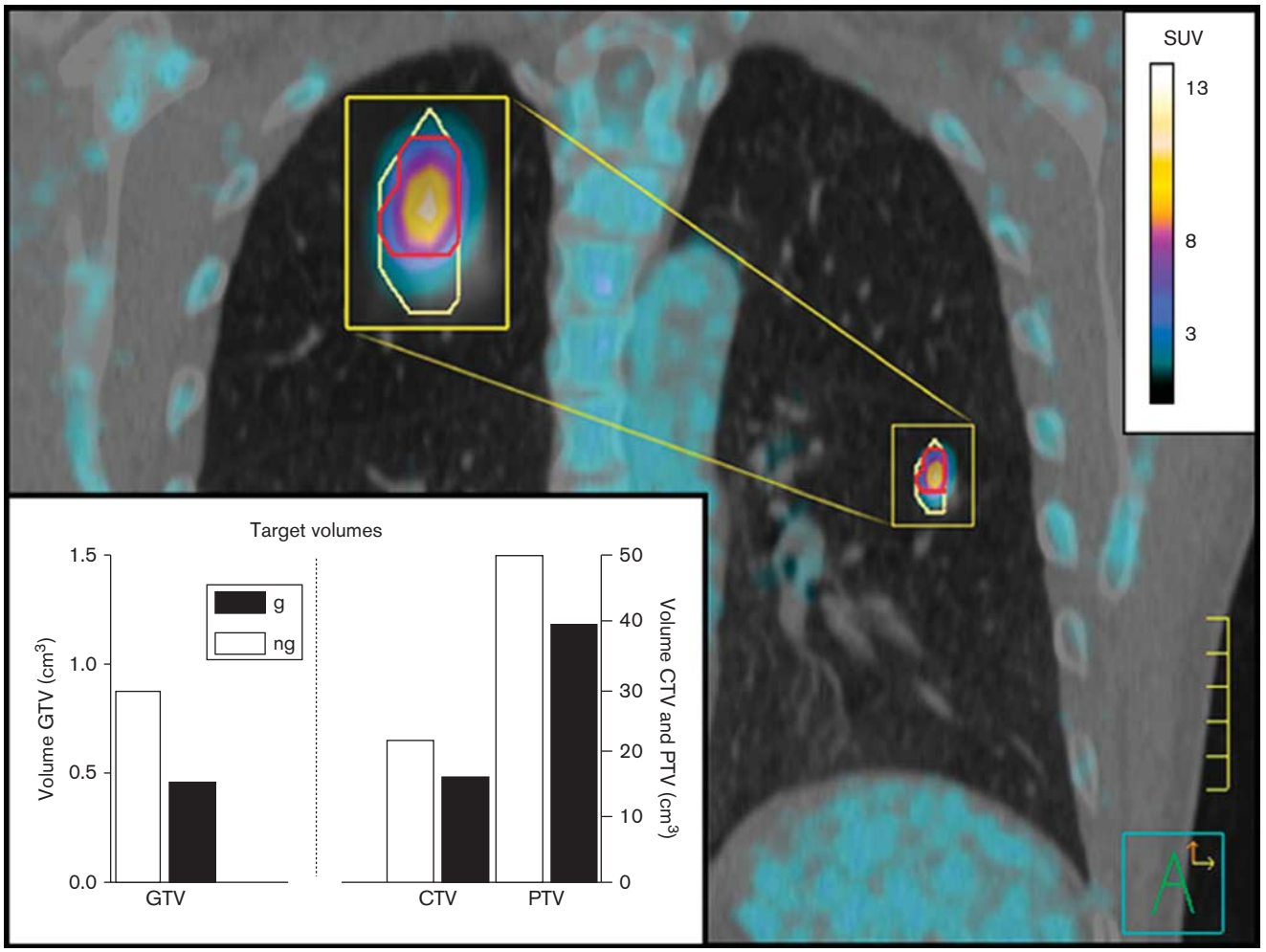

Target volume reduction: a clinical example. An optimally gated fluorine-18 fluorodeoxyglucose PET image (fused with the accompanying low-dose computed tomography) showing a remarkable reduction in gated (g) gross tumour volume (GTV, red; 0.45 cm^3) compared with the nongated (ng) GTV (yellow; 0.87 cm^3). The bar graph shows both the nongated and gated GTV, clinical target volume (CTV) and planning target volume (PTV) for this patient. SUV, standaradized uptake value.

mean dose to the organ at risk (D_{mean}) and the percentage of an organ exceeding a certain dose (for example 20% of the lung receiving 5 Gy or more, denoted as $V_{5lung} = 20\%$). The latter was done for organ volumes receiving doses from 5 to 70 Gy with 5 Gy intervals. The isodose lines (range 5 to 70 Gy, again with 5 Gy intervals) were converted into contours; thus, the actual volume (cm^3) of an organ receiving a certain radiation dose was calculated.

The study was carried out in accordance with the national applicable rules on the review of research ethics committees and informed consent.

Statistics

All statistical analyses were carried out using the Wilcoxon signed-rank test for paired variables (SPSS software, version 20.0; SPSS Inc., Chicago, Illinois, USA). A *P*-value of less than 0.05 was considered statistically significant. The reported *P*-values are adjusted for multiple testing using the Bonferroni correction.

Results

As reported by Grootjans *et al.* [18], optimally respiratory gated ^{18}F-FDG-PET resulted in a significant increase in SUV_{mean} (mean standardized uptake value), with a concomitant significant decrease in lesion volume. The latter was also true for our results as all except two of the gated GTVs were smaller compared with the nongated GTVs (Table 1). The median volumes of GTVg, CTVg and PTVg [4.6 cm^3 interquartile range (IQR) 2.2–13.9, 50.8 cm^3 (32.8–109.6) and 99.8 cm^3 (70.7–189.8), respectively] were statistically significantly smaller compared with the corresponding nongated

Table 1 Volumes (cm^3) of the individual target volumes (22 primary NSCLC in 21 patients)

	GTVng	GTVg	ΔGTV	%ΔGTV	CTVng	CTVg	ΔCTV	%ΔCTV	PTVng	PTVg	ΔPTV	%ΔPTV
Upper lobe												
Right	6.63	5.38	−1.25	−18.85	41.94	35.14	−6.80	−16.21	87.21	74.56	−12.65	−14.51
Right	14.86	13.04	−1.82	−12.25	111.10	107.69	−3.41	−3.07	191.23	186.42	−4.81	−2.52
Right	2.94	2.78	−0.16	−5.44	50.76	53.43	2.67	5.26	102.15	107.20	5.05	4.94
Right	2.79	2.30	−0.49	−17.56	29.07	28.73	−0.34	−1.17	63.71	62.69	−1.02	−1.60
Left	8.79	8.15	−0.64	−7.28	67.74	66.04	−1.70	−2.50	125.55	123.02	−2.53	−2.02
Left	3.60	3.51	−0.09	−2.50	33.53	34.12	0.59	1.76	71.83	73.31	1.48	2.06
Left	1.54	1.47	−0.07	−4.55	19.71	19.92	0.21	1.07	47.70	48.45	0.75	1.57
Left	1.28	1.19	−0.09	−7.03	19.88	20.05	0.17	0.86	48.01	48.37	0.36	0.75
Hilum												
Right	26.95	23.26	−3.69	−13.69	154.08	146.34	−7.74	−5.00	256.48	245.30	−11.18	−4.36
Right	4.98	3.74	−1.24	−24.90	56.96	49.45	−7.51	−13.18	109.41	97.79	−11.62	−10.62
Right	35.56	25.58	−9.98	−28.07	217.23	188.02	−29.21	−13.45	348.71	309.45	−39.26	−11.26
Left	6.87	6.20	−0.67	−9.75	61.69	61.10	−0.59	−0.96	115.15	114.70	−0.45	−0.39
Left	9.39	8.83	−0.56	−5.96	71.01	68.68	−2.33	−3.28	140.73	136.59	−4.14	−2.90
Left	27.03	27.07	0.04	0.15	129.61	128.23	−1.38	−1.10	213.86	211.89	−1.97	−0.90
Lower lobe												
Right	8.87	7.78	−1.09	−12.29	54.79	52.18	−2.61	−4.76	105.26	101.73	−3.53	−3.35
Right	16.93	16.28	−0.65	−3.84	115.25	115.18	−0.07	−0.06	199.74	199.98	0.24	0.12
Right	2.47	2.03	−0.44	−17.81	45.48	35.76	−9.72	−21.37	94.02	77.23	−16.79	−17.86
Right	1.42	1.55	0.13	9.15	23.05	25.59	2.54	11.02	53.06	57.55	4.49	8.46
Left	0.87	0.45	−0.42	−48.28	21.43	15.82	−5.61	−26.18	49.62	39.12	−10.50	−21.16
Left	3.91	3.38	−0.53	−13.55	37.08	37.84	0.76	2.05	76.75	77.78	1.03	1.34
Left	3.05	2.57	−0.48	−15.74	40.71	39.50	−1.21	−2.97	82.57	81.10	−1.47	−1.78
Left	78.53	72.38	−6.15	−7.80	297.20	288.66	−8.54	−2.90	459.58	447.68	−11.90	−2.59

Δ and %Δ mark the absolute and relative differences between gated and nongated target volumes, respectively.
A negative sign represents a volume reduction in favour of the gated target volume.
CTV, clinical target volume; g, gated; GTV, gross tumour volume; ng, nongated; NSCLC, non-small-cell lung cancer; PTV, planning target volume.

volumes [5.8 cm^3 (2.7–15.4), 52.8 cm^3 (32.4–112.1) and 103.7 cm^3 (69.8–193.4); $P = 0.003$, 0.021 and 0.036, respectively]. This resulted in a median target volume reduction of 0.5 cm^3 (IQR 0.1–1.2), 1.5 cm^3 (−0.2 to 7.0) and 2.3 cm^3 (−0.5 to 11.3) for the GTVg, CTVg and PTVg, respectively (Fig. 2).

Subsequently, we analysed the effect of these smaller target volumes on the radiation doses to the OARs. Only the volume of lung (GTV included) receiving at least 35 Gy was significantly smaller for the treatment plans with the gated target volumes [median volume 265 cm^3 (gated) versus 284 cm^3 (nongated); $P = 0.048$]. This corresponded to a median difference in lung volume of 5.7 cm^3 (IQR −0.8 to 30.5), comprising 0.15% of the median total lung volume. Dose distributions for the lung minus GTV and the other OAR did not show any significant difference (Fig. 3). Dose coverages for PTVng and PTVg were identical (the median coverage by the 95% isodose was 99% for both PTVs; $P = 0.878$).

We repeated the analysis taking into account anatomical differences that may influence tumour motion. Three subgroups were defined (upper lobes, lung hilum and lower lobes), showing only the gated upper lobe GTVs to be significantly smaller. The differences were small, with a median volume of the gated upper and lower lobe GTVs of 3.1 cm^3 (IQR 1.7–7.5) and 3.0 cm^3 (1.7–14.2), respectively, compared with the respective nongated GTVs [3.3 cm^3 (1.9–8.3) and 3.5 cm^3 (1.7–14.9); $P = 0.036$ and 0.051, respectively]. No statistically significant reductions in the median volume of the upper lobe CTVs (nongated 37.7 cm^3 versus gated 34.6 cm^3; $P = 1.0$), lower lobe CTVs (nongated 43.1 cm^3 versus gated 38.7 cm^3; $P = 0.28$), upper lobe PTVs (nongated 79.5 cm^3 versus gated 73.9 cm^3; $P = 1.0$) and lower lobe PTVs (nongated 88.3 cm^3 versus gated 79.4 cm^3; $P = 1.0$) were found. Accordingly, no significant differences in dose volume distribution could be identified.

Discussion

The incorporation of optimally respiratory gated ^{18}F-FDG-PET imaging into radiotherapy planning for NSCLC shows that the acquired gated GTVs, CTVs and PTVs are significantly smaller, however, without the desirable relevant reduction of radiation dose to the OAR. Although the lung volume receiving at least 35 Gy (V_{35lung}) was significantly smaller for the gated ^{18}F-FDG-PET planned treatment plans, the actual median V_{35lung} reduction was minimal. The evaluation of tumour localization on target volume resulted in smaller GTVs for the upper lobes, but again, without any effect on the corresponding dose distributions.

Although smaller target volumes are generated using gated ^{18}F-FDG-PET, the expected beneficial effect on treatment planning was small. This is indicated by the fact that only one isodose level appeared to be significantly different, showing a relative decrease in volume of the lung receiving at least 35 Gy of only 0.15%. Albeit statistically significant, this small decrease in radiation exposure to healthy lung tissue is most likely clinically irrelevant.

Fig. 2

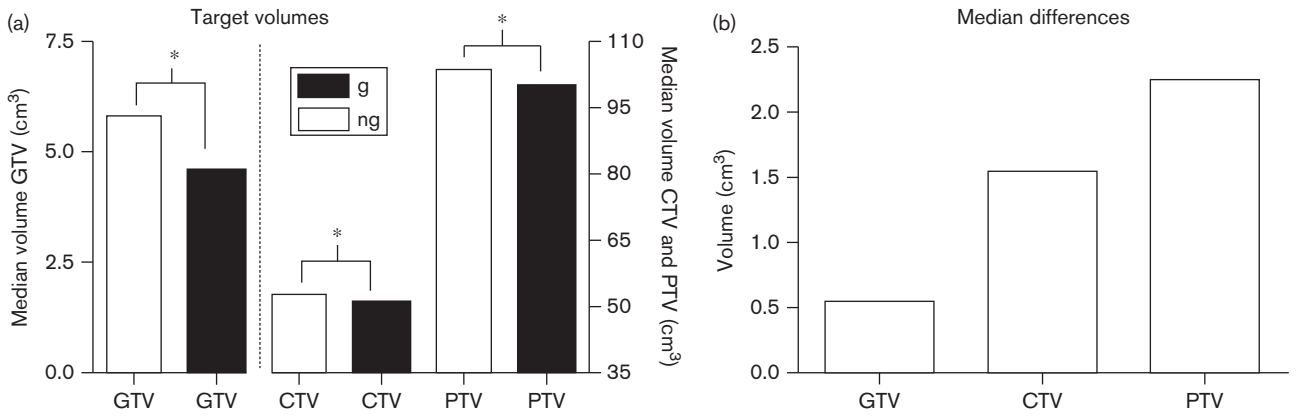

Bar graphs showing the median target volume reduction. (a) Median volumes of the nongated (ng) and gated (g) gross tumour volume (GTV), clinical target volume (CTV) and planning target volume (PTV). (b) Median differences (ng volume − g volume) for GTV, CTV and PTV. *Statistically significant.

The explanation for the discrepancy between reduced target volumes with almost no gain in radiotherapy planning lies in the fact that the absolute reduction in target volume is small. This might be a result of the method that we used for gating as the software identifies the smallest amplitude range of the respiratory signal while still using 35% of the total acquired PET data (duty cycle). This 'movement-weighted' approach often selects the ^{18}F-FDG-PET data from the end-expiration phase to reconstruct the image [17]. Notwithstanding that reduction of tumour motion is achieved, residual tumour motion may still be present. This residual tumour motion still causes blurring of the ^{18}F-FDG-PET image, diminishing the potential reduction in target volume. Another physical aspect is the wider photon beam penumbra in lung tissue. Because of extended electron ranges in lung tissue, the distance from beam edge to target volume increases to achieve full dose coverage of the target volume. From our results, the target volume reduction is apparently not large enough to compensate for this. Moreover, the applied identification of the 40% SUV_{max} by means of interpolation of pixel values may not be optimal. Compared with pixel-per-pixel delineated volumes, this interpolation of pixels at the border of the 40% SUV_{max} volume may possibly increase the delineated volume.

Although a limited number of tumours has been assessed, increasing the number of patients studied will most probably not significantly increase the differences in radiation dose to the OAR. This is because the tumours have been selected beforehand as they showed the largest reduction in gated tumour volumes compared with the corresponding nongated volumes.

After sorting the tumours according to localization within the lungs, the reduction in CTV and PTV lost significance. This is counterintuitive as one may expect a larger effect on lower lobe tumours compared with upper lobe tumours as tumour movement has been shown to be larger for that lung subvolume [20]. The loss of significance is probably because of the avoidance of healthy tissue when the CTV is created by circumferential expansion of the GTV. Furthermore, as the GTV shape is often irregular, circumferential expansion of such an irregular GTV (resembling for example a horseshoe figure) creates a sphere like CTV, resulting in a (partial) loss of the target volume reduction achieved with respiratory gating.

The target volumes created with gated ^{18}F-FDG-PET were the subject of investigation in two other studies. Guerra *et al.* [21] analysed 13 lung cancer patients undergoing a free-breathing CT together with a gated ^{18}F-FDG-PET/CT. The latter was reconstructed into six breathing phases used for the delineation of one internal target volume (ITV). Despite the fact that the ITVs were significantly increased using gated ^{18}F-FDG-PET/CT, the accompanying PTVs were significantly reduced. This unexpected result can be explained by the different expansion margins used: a 10 mm circumferential margin for free-breathing target volumes versus anisotropic margins of 7–8 and 5 mm for gated target volumes. Indeed, a target volume margin reduction may be appropriate as tumour motion is already (in part) incorporated into the CTV. However, it remains unclear whether or not the smaller PTVs are because of this margin reduction, the use of gated imaging or a combination of both. For this reason, we decided to apply equal margins for nongated and gated treatment plans as only the added value of gated ^{18}F-FDG-PET was under investigation, not the delivery of gated radiotherapy. Aristophanous *et al.* [22] evaluated 22 lung tumours in 10 patients undergoing gated ^{18}F-FDG-PET/CT imaging before radiotherapy. The mean gated target volume was

Fig. 3

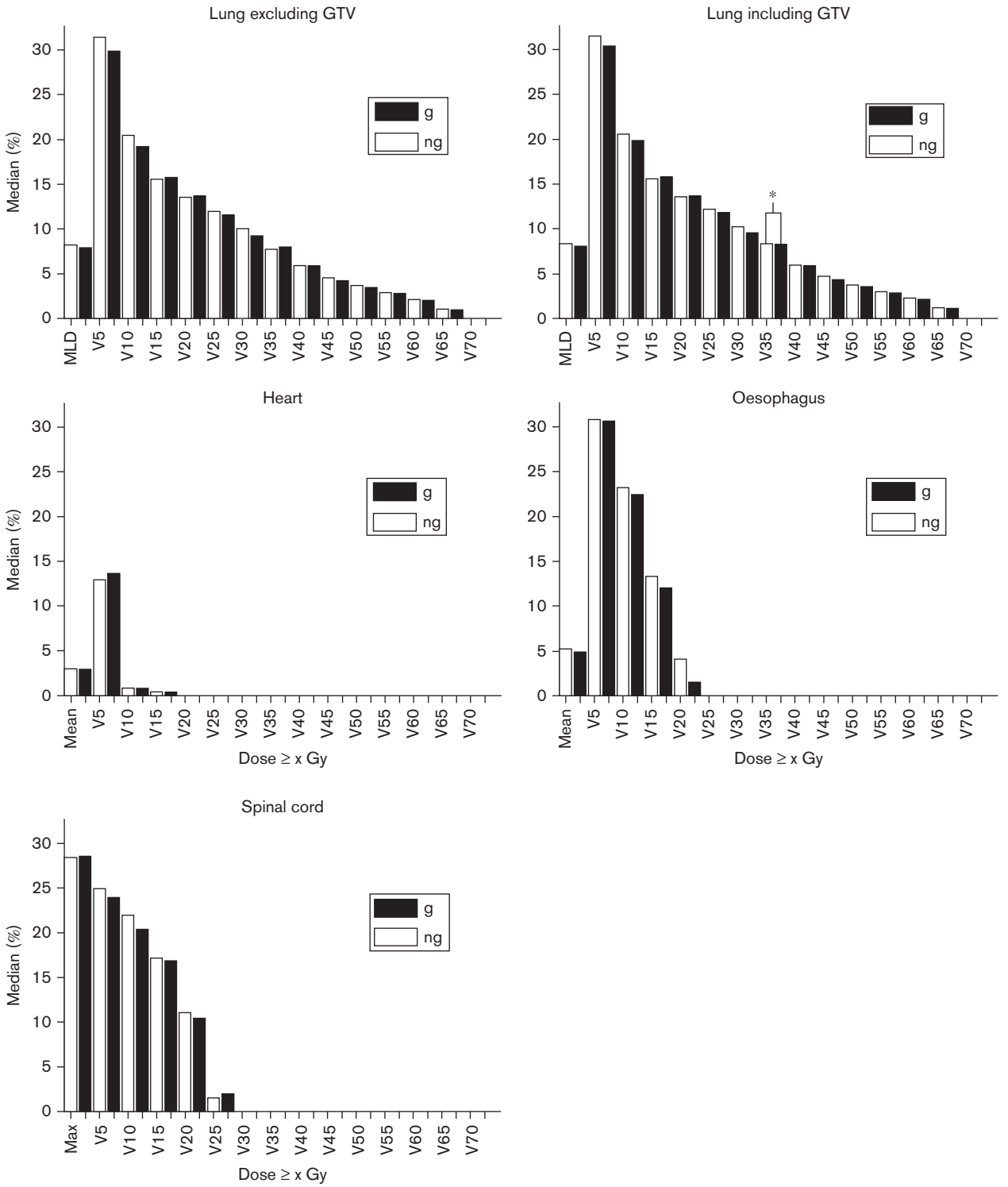

Effect of target volume reduction on the dose distributions for the organs at risk. The bar graphs show the paired (ng = nongated and g = gated) median volume percentages of a certain dose level for the specific organ at risk (e.g. V_5 indicates percentage receiving ≥ 5 Gy). GTV, gross tumour volume; MLD, mean lung dose. *Statistically significant.

35% larger compared with the nongated target volume, with the lower lobe target volumes showing a more pronounced increase compared with the upper lobe target volumes. In both the above-mentioned studies, the ITV concept was applied. This concept considers the extreme ends of tumour motion to be the boundary of the GTV, which often results in overestimation of the target volume as the tumour is located relatively short in that extreme position during the breathing cycle [23]. Without being at the expense of good dose coverage, this overestimation can be decreased by avoiding the incorporation of the extreme ends of tumour motion using an average position method as described by Wolthaus *et al.* [23]. Although not yet evaluated, our method of GTV delineation using optimally respiratory gated ^{18}F-FDG-PET may be considered such an average position approach. This explains the fact that, compared with the ITV concept, our target volumes are on average reduced instead of increased as the incorporation of the extreme ends of tumour motion is avoided.

In our study, we not only analysed the target volumes created with gated ^{18}F-FDG-PET imaging but also evaluated the actual impact on the dose distributions with respect to the radiation doses for the OAR, the latter being of special interest in, for example, radiation dose-escalation strategies to the entire tumour volume where the avoidance of high dose to healthy tissues is of utmost importance. Although the incorporation of gated PET into radiation therapy planning failed to show clinically relevant dose reductions for the OAR in our study, it may still be useful in defining biologically unfavourable subvolumes within the GTV that are suitable for dose painting as the true tumour volume and tracer uptake can be more accurately assessed with gated PET [24].

Instead of the commonly used 40% SUV_{max}, one may consider different thresholds or other segmentation techniques. However, there is no consensus on the optimal segmentation technique. Although one may suggest using, for example, probabilistic or gradient-based approaches to reduce the influence of partial volume effects, the partial volume effect is small in our scans as we applied high-resolution PET with a matrix size of 400 ×400 (pixel spacing of 2.04 mm). Furthermore, the autosegmentations were visually checked for plausibility; hence, major delineation inconsistencies are unlikely. Because our primary goal was to evaluate the impact of gated PET on treatment planning and its theoretical sparing of healthy tissues, we studied only one segmentation method, not the differences between segmentation methods *per se*. The methodology that we applied may have introduced a mismatch in attenuation correction because a phase-matched low-dose CT for attenuation correction of the gated ^{18}F-FDG-PET was not available. We used the nongated low-dose CT for this purpose instead, which may result in a small bias in PET data. This is a subject of further research at our institution.

Conclusion

This study evaluated the impact of optimally respiratory gated ^{18}F-FDG-PET on radiotherapy target volumes including the effect on radiotherapy planning and the radiation doses for healthy tissues. Although the respiratory gated target volumes were reduced, the benefit in this selected group of NSCLC patients was too small to show clinically significant dose reduction for the healthy tissues.

Acknowledgements

Conflicts of interest

W. Grootjans received an educational grant from Siemens Healthcare, The Hague, The Netherlands, during the conduct of the study. E. Van der Heijden reports grants from Pentax Medical Systems, personal fees and other from Lilly Oncology, other from Pfizer Oncology, other from MediGlobe, all outside the scope of this submitted research. For the remaining authors there are no conflicts of interest.

References

1 Detterbeck FC, Boffa DJ, Tanoue LT. The New Lung Cancer Staging System. *Chest* 2009; **136**:260–271.
2 Auperin A, Le Pechoux C, Rolland E, Curran WJ, Furuse K, Fournel P, *et al.* Meta-analysis of concomitant versus sequential radiochemotherapy in locally advanced non-small-cell lung cancer. *J Clin Oncol* 2010; **28**:2181–2190.
3 Cox JD. Are the results of RTOG 0617 mysterious? *Int J Radiat Oncol Biol Phys* 2012; **82**:1042–1044.
4 Grills IS, Yan D, Martinez AA, Vicini FA, Wong JW, Kestin LL. Potential for reduced toxicity and dose escalation in the treatment of inoperable non-small-cell lung cancer: a comparison of intensity-modulated radiation therapy (IMRT), 3D conformal radiation, and elective nodal irradiation. *Int J Radiat Oncol Biol Phys* 2003; **57**:875–890.
5 Jiang X, Li T, Liu Y, Zhou L, Xu Y, Zhou X, *et al.* Planning analysis for locally advanced lung cancer: dosimetric and efficiency comparisons between intensity-modulated radiotherapy (IMRT), single-arc/partial-arc volumetric modulated arc therapy (SA/PA-VMAT). *Radiat Oncol* 2011; **6**:140–147.
6 Schwarz M, Alber M, Lebesque JV, Mijnheer BJ, Damen EM. Dose heterogeneity in the target volume and intensity-modulated radiotherapy to escalate the dose in the treatment of non-small-cell lung cancer. *Int J Radiat Oncol Biol Phys* 2005; **62**:561–570.
7 Govaert SL, Troost EG, Schuurbiers OC, de Geus-Oei LF, Termeer A, Span PN, *et al.* Treatment outcome and toxicity of intensity-modulated (chemo) radiotherapy in stage III non-small cell lung cancer patients. *Radiat Oncol* 2012; **7**:150–156.
8 Hoffmann AL, Troost EG, Huizenga H, Kaanders JH, Bussink J. Individualized dose prescription for hypofractionation in advanced non-small-cell lung cancer radiotherapy: an in silico trial. *Int J Radiat Oncol Biol Phys* 2012; **83**:1596–1602.
9 Bradley J, Bae K, Choi N, Forster K, Siegel BA, Brunetti J, *et al.* A phase II comparative study of gross tumor volume definition with or without PET/CT fusion in dosimetric planning for non-small-cell lung cancer (NSCLC): primary analysis of Radiation Therapy Oncology Group (RTOG) 0515. *Int J Radiat Oncol Biol Phys* 2012; **82**:435.e1–441 e1.
10 Cheebsumon P, Boellaard R, de Ruysscher D, van Elmpt W, van Baardwijk A, Yaqub M, *et al.* Assessment of tumour size in PET/CT lung cancer studies: PET- and CT-based methods compared to pathology. *EJNMMI Res* 2012; **2**:56.
11 van Baardwijk A, Bosmans G, Boersma L, Buijsen J, Wanders S, Hochstenbag M, *et al.* PET-CT-based auto-contouring in non-small-cell lung cancer correlates with pathology and reduces interobserver variability in the delineation of the primary tumor and involved nodal volumes. *Int J Radiat Oncol Biol Phys* 2007; **68**:771–778.
12 Usmanij EA, de Geus-Oei LF, Troost EG, Peters-Bax L, van der Heijden EH, Kaanders JH, *et al.* ^{18}F-FDG PET early response evaluation of locally advanced non-small cell lung cancer treated with concomitant chemoradiotherapy. *J Nucl Med* 2013; **54**:1528–1534.

13 Wijsman R, Kaanders JH, Oyen WJ, Bussink J. Hypoxia and tumor metabolism in radiation oncology: targets visualized by positron emission tomography. *Q J Nucl Med Mol Imaging* 2013; **57**:244–256.
14 Aerts HJ, van Baardwijk AA, Petit SF, Offermann C, Loon J, Houben R*, et al*. Identification of residual metabolic-active areas within individual NSCLC tumours using a pre-radiotherapy (18)fluorodeoxyglucose-PET-CT scan. *Radiother Oncol* 2009; **91**:386–392.
15 Bettinardi V, Picchio M, Di Muzio N, Gilardi MC. Motion management in positron emission tomography/computed tomography for radiation treatment planning. *Semin Nucl Med* 2012; **42**:289–307.
16 Nehmeh SA, Erdi YE. Respiratory motion in positron emission tomography/computed tomography: a review. *Semin Nucl Med* 2008; **38**:167–176.
17 van Elmpt W, Hamill J, Jones J, De Ruysscher D, Lambin P, Ollers M. Optimal gating compared to 3D and 4D PET reconstruction for characterization of lung tumours. *Eur J Nucl Med Mol Imaging* 2011; **38**:843–855.
18 Grootjans W, de Geus-Oei LF, Meeuwis AP, van der Vos CS, Gotthardt M, Oyen WJ*, et al*. Amplitude-based optimal respiratory gating in positron emission tomography in patients with primary lung cancer. *Eur Radiol* 2014; **24**:3242–3250.
19 Erdi YE, Mawlawi O, Larson SM, Imbriaco M, Yeung H, Finn R*, et al*. Segmentation of lung lesion volume by adaptive positron emission tomography image thresholding. *Cancer* 1997; **80**:2505–2509.
20 Seppenwoolde Y, Shirato H, Kitamura K, Shimizu S, van Herk M, Lebesque JV*, et al*. Precise and real-time measurement of 3D tumor motion in lung due to breathing and heartbeat, measured during radiotherapy. *Int J Radiat Oncol Biol Phys* 2002; **53**:822–834.
21 Guerra L, Meregalli S, Zorz A, Niespolo R, De Ponti E, Elisei F*, et al*. Comparative evaluation of CT-based and respiratory-gated PET/CT-based planning target volume (PTV) in the definition of radiation treatment planning in lung cancer: preliminary results. *Eur J Nucl Med Mol Imaging* 2014; **41**:702–710.
22 Aristophanous M, Berbeco RI, Killoran JH, Yap JT, Sher DJ, Allen AM*, et al*. Clinical utility of 4D FDG-PET/CT scans in radiation treatment planning. *Int J Radiat Oncol Biol Phys* 2012; **82**:e99–e105.
23 Wolthaus JW, Sonke JJ, van Herk M, Belderbos JS, Rossi MM, Lebesque JV*, et al*. Comparison of different strategies to use four-dimensional computed tomography in treatment planning for lung cancer patients. *Int J Radiat Oncol Biol Phys* 2008; **70**:1229–1238.
24 Aristophanous M, Yap JT, Killoran JH, Chen AB, Berbeco RI. Four-dimensional positron emission tomography: implications for dose painting of high-uptake regions. *Int J Radiat Oncol Biol Phys* 2011; **80**:900–908.